



Research article

The influence of meteorological variables on CO₂ and CH₄ trends recorded at a semi-natural station



Isidro A. Pérez^{*}, M. Luisa Sánchez, M. Ángeles García, Nuria Pardo, Beatriz Fernández-Duque

Department of Applied Physics, Faculty of Sciences, University of Valladolid, Paseo de Belén, 7, 47011 Valladolid, Spain

ARTICLE INFO

Article history:

Received 29 May 2017

Received in revised form

8 November 2017

Accepted 11 December 2017

Keywords:

Carbon dioxide

Methane

GHG trend

Air parcel trajectory

METEX

ABSTRACT

CO₂ and CH₄ evolution is usually linked with sources, sinks and their changes. However, this study highlights the role of meteorological variables. It aims to quantify their contribution to the trend of these greenhouse gases and to determine which contribute most. Six years of measurements at a semi-natural site in northern Spain were considered. Three sections are established: the first focuses on monthly deciles, the second explores the relationship between pairs of meteorological variables, and the third investigates the relationship between meteorological variables and changes in CO₂ and CH₄. In the first section, monthly outliers were more marked for CO₂ than for CH₄. The evolution of monthly deciles was fitted to three simple expressions, linear, quadratic and exponential. The linear and exponential are similar, whereas the quadratic evolution is the most flexible since it provided a variable rate of concentration change and a better fit. With this last evolution, a decrease in the change rate was observed for low CO₂ deciles, whereas an increasing change rate prevailed for the rest and was more accentuated for CH₄. In the second section, meteorological variables were provided by a trajectory model. Backward trajectories from 1-day prior to reaching the measurement site were used to calculate distance and direction averages as well as the recirculation factor. Terciles of these variables were determined in order to establish three intervals with low, medium and high values. These intervals were used to classify the variables following their interval widths and skewnesses. The best correlation between pairs of meteorological variables was observed for the average distance, in particular with horizontal wind speed. Sinusoidal relationships with the average direction were obtained for average distance and for vertical wind speed. Finally, in the third section, the quadratic evolution was considered in each interval of all the meteorological variables. As regards the main result, the greatest increases were obtained for high potential temperature for both gases followed by low and medium boundary layer height for CO₂ and CH₄, respectively. Combining both meteorological variables provided increases of 22 ± 9 and 0.070 ± 0.019 ppm for CO₂ and CH₄, respectively, although the number of observations affected is small, around 7%.

© 2017 Elsevier Ltd. All rights reserved.

1. Introduction

Interest in the evolution of GHG has increased in recent years. Indeed, they are systematically measured at remote locations around the world (WDCGG, 2017). Buchholz et al. (2016) consider that developing policies to control air quality should take into account meteorological conditions. Most analyses highlight the role of sources and sinks whereas few studies have explored the

relationship between GHG and meteorological variables (Sreenivas et al., 2016), whilst some focus on local effects, such as recirculation over complex terrain (Kutter et al., 2017), or micrometeorological observations of atmospheric stable stratification (Wharton et al., 2017). The present paper goes a step further since it focuses on meteorological variables and seeks to investigate the conditions that favour the most marked CO₂ and CH₄ evolution.

The evolution of CO₂ and CH₄ has often been described by composite equations comprising two parts (Fernández-Duque et al., 2017; Pérez et al., 2017), one being harmonic to include daily and yearly cycles, which lies outside the scope of this study, and the other being responsible for the concentration trend.

^{*} Corresponding author.

E-mail address: iaperez@fa1.uva.es (I.A. Pérez).

Most authors describe GHG evolution by a linear expression (Eneroth et al., 2005; Timokhina et al., 2015; Wu et al., 2012), since it is simple and provides an accurate value of the trend. Other studies consider second order polynomials (Fang et al., 2016) whilst only a few include higher order polynomials (Inoue et al., 2006). The first objective of this paper is to quantify simple equations, which are the expressions currently used to describe the concentration evolution. One main difference between this analysis and previous studies is that these equations are compared in order to choose the one that provides the best fit.

The second objective is to explore the influence of meteorological variables on CO₂ and CH₄ evolution in order to establish the conditions that lead to major increases in the two trace gases. CO₂ and CH₄ response to meteorological variables has previously been explored (García et al., 2012; Pérez et al., 2016; Sánchez et al., 2010). However, the relationship between the concentration trend and meteorological variables is not common and requires more detailed research.

In order to obtain the meteorological variables, an air trajectory model has been used. These models have multiple applications in the field of atmospheric science (Pérez et al., 2015a) and their use has increased in recent years. Their main advantage is that the air parcel trajectory provides information beyond the local range, whereas in situ measurements are influenced by surrounding features such as small hills or changes in surface that disturb airflow (Grant et al., 2015). Moreover, use of the air trajectory model has been favoured by the development of web-based versions such as those of the National Oceanic and Atmospheric Administration (NOAA, 2017) or the Centre for Global Environmental Research (CGER, 2017), which enable air parcel evolution at different sites, times, and heights to be obtained more quickly and with varied temporal extensions.

In this study, meteorological variables are first considered separately so as gain a clearer idea of their distribution, although relationships between pairs are subsequently investigated. A key feature of this analysis is the inclusion of trajectory variables such as the recirculation factor, which are rarely considered, in addition to the usual meteorological variables.

Hernández-Paniagua et al. (2015) calculated the annual CO₂ rate for wind direction sectors in southwest London. This paper follows that analysis, although with two major differences. The first is the greater number of meteorological variables considered, in an effort to quantify the trend linked to each variable. The second difference is the number of intervals proposed for each variable. This study considers a low number of intervals so as to retain sufficient observations when pairs of variables are combined.

Finally, key points of this study are the detailed quantification of the CO₂ and CH₄ trend and proposing the most relevant meteorological variables for their evolution.

2. Materials and methods

2.1. Measurement campaign

Measurements were carried out at the Low Atmosphere Research Centre, CIBA (41° 48' 50.26" N, 4° 55' 58.53" W, 852 m a.s.l.) over six years, commencing on 15 October 2010. The site is nearly flat, with Mediterranean shrubland being the main vegetation.

CO₂ and CH₄ dry concentrations were measured with a Picarro G1301, which recorded them at 1.8, 3.7 and 8.3 m above ground level every 10 min at each level, and half-hour averages were systematically calculated. Since no statistical differences were found between the three levels (Fernández-Duque et al., 2017), only measurements taken at the 1.8 m level, the one most affected by the

ground, are considered in this paper. The device functioned correctly, although 16.3% of observations were missing due to maintenance.

The METeorological data EXplorer, METEX (Zeng et al., 2010), was used to calculate air trajectories, its most noticeable feature being the small number of specifications required. It was recently applied to investigate the air mass origin affecting CO₂ concentrations recorded at Mt. Fuji (Nomura et al., 2017). In this study, calculations were performed every year. The kinematic model, which considers that an air parcel trajectory is given by the horizontal wind components and vertical pressure velocity, was selected. The interval between consecutive trajectories was 1 h, and 1-day backward trajectories at 500 m a.g.l. at the study site were considered. Moreover, this model provided ancillary meteorological variables such as the boundary layer height, u , v and w components of wind speed (the first two were combined to obtain horizontal wind speed), potential temperature and pressure. Since the lowest time resolution of this model is one hour, concentrations were averaged to combine them with the METEX values.

2.2. Trajectory calculations

Fig. 1a presents a 1-day backward trajectory reaching CIBA, point A, from point B. Black points correspond to hourly positions of the air parcel. The average distances d_i from each hourly position to the arrival point were calculated for every trajectory. Directions θ_i were decomposed into their sine and cosine components, which were added and then composed to obtain the average direction. The recirculation factor, R , was calculated following Allwine and Whiteman (1994), defining the wind run, S , as the total distance travelled by the air parcel

$$S = \sum_{i=1}^{24} S_i \quad (1)$$

where S_i is the distance between consecutive hourly positions. These distances are arcs on the Earth's surface which may be calculated using the Sinnott equation and the Earth's radius (Snyder, 1987). The resulting transport distance, L , is the minimum distance between the beginning of the trajectory, point B, and the end, point A. The recirculation factor, R , may then be calculated.

$$R = 1 - \frac{L}{S}. \quad (2)$$

Fig. 1b was drawn so as to obtain a visual representation of this factor. Trajectories are considered as arcs of circumferences. The distance between A and B is L , the chord of a circumference of centre C and radius r , whose arc is S . The relationship between L , S and its corresponding angle α is

$$\frac{L}{2S} \alpha = \sin \frac{\alpha}{2}, \quad (3)$$

which must be solved numerically. A recirculation factor of about 0.36 is obtained when the AB distance is the diameter of the circumference.

2.3. Statistics

Eight meteorological variables were considered. Three were calculated for each 1-day backward trajectory. These were distance and direction averages, and the recirculation factor. The rest are variables provided at the arrival site. This group is formed by boundary layer height, horizontal and vertical wind speed,

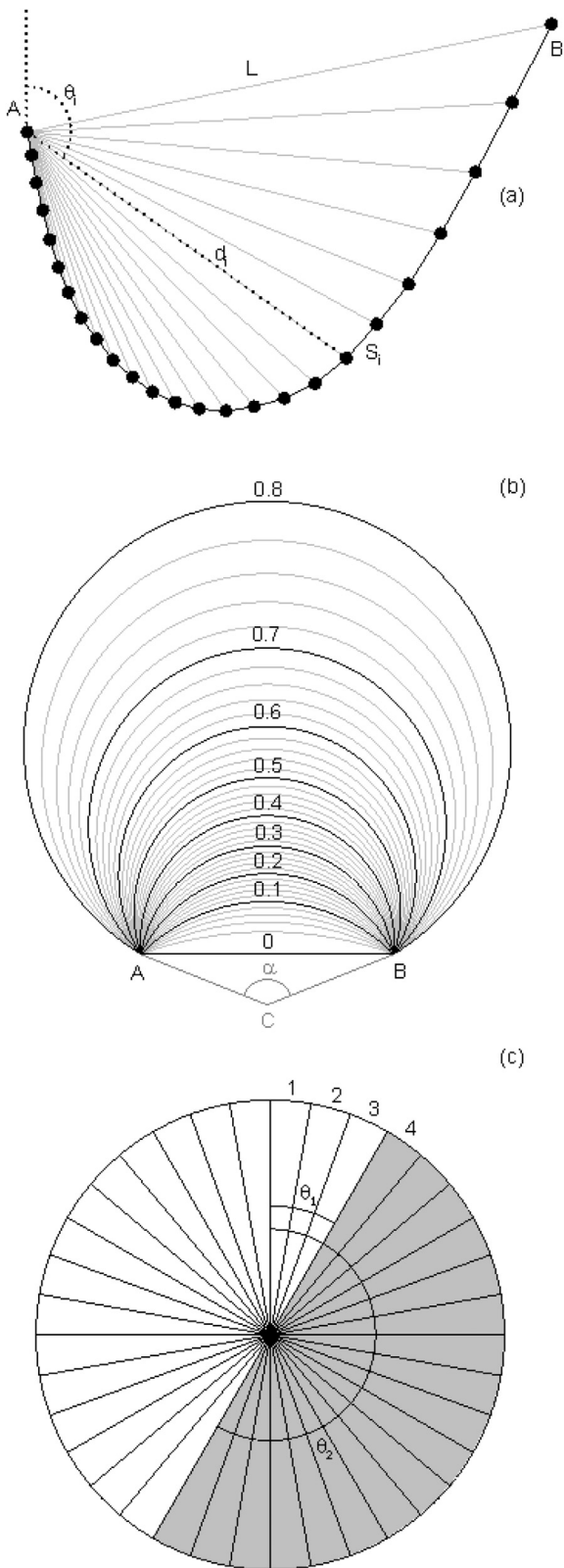


Fig. 1. Schemes showing (a) 1-day backward trajectory reaching A, (b) circumference arcs corresponding to different recirculation parameters, and (c) sectors used to obtain the median direction.

potential temperature and pressure.

Each variable was ordered and three groups with the same number of observations were formed. Obtaining these terciles is straightforward for linear variables. However, calculating them for angular variables, such as the direction average, requires further development. Fisher (1993) defined the median direction for circular variables as the direction θ that minimises the function

$$D(\theta) = \pi - \frac{1}{n} \sum_{i=1}^n \left| \pi - \left| \bar{\theta}_i - \theta \right| \right|, \quad (4)$$

where n is the number of 1-day backward trajectories and $\bar{\theta}_i$ each average direction. This calculation may be easily performed when the number of observations is small. However, obtaining a median may require a great deal of time and use of extensive datasets. This inconvenience may be overcome with an approximate value, which is accurate enough for most applications. The procedure was used by Pérez et al. (2014) for linear variables. The first step towards reaching this approximate value is to build the histogram by binning observations. Narrow bins lead to a value close to the median. Fig. 1c considers 36 bins to illustrate the procedure, although 3600 bins were used with the experimental dataset. The first four bins were numbered. Secondly, observations in consecutive bins for a π radian angle were counted. In Fig. 1c, observations in the shaded area are assigned to bin 4. This addition is calculated for each bin. The value closest to 50% corresponds to the median direction. However, two directions differing in π radians are possible, which are represented by directions θ_1 and θ_2 in Fig. 1c. The median corresponds to the direction where observations are most grouped. Equation (4) was used with both directions, with the value that provides the lowest quantity for this equation being selected as the median and the opposite as the origin. Once the median is determined, observations of bins counter-clockwise from the median are added to reach 16.67% so as to obtain the 1st tercile, and observations of bins clockwise from the median are considered up to 16.67% in order to obtain the 2nd tercile. This procedure is similar to that presented by Abuzaid et al. (2012) to calculate 1st and 3rd quartiles.

The easiest way to investigate the relationship between one linear variable X and one angular variable θ is by considering a linear equation in the variables $\cos \theta$ and $\sin \theta$. A measure of this dependence was presented by Mardia (1976) by

$$R^2 = \left(r_1^2 + r_2^2 - 2r_1r_2r_3 \right) / \left(1 - r_3^2 \right), \quad (5)$$

where r_1 is the Pearson correlation coefficient between X_i and $\cos \theta_i$, and r_2 and r_3 correspond to correlations between X_i and $\sin \theta_i$, and $\cos \theta_i$ and $\sin \theta_i$, respectively.

2.4. Equations of trend

Closed-form expressions were used to fix the evolutions. A straight line is the simplest way to detect a trend (Angelbratt et al., 2011),

$$y = a_1 + a_2t, \quad (6)$$

where t is the time from when measuring commences and y the corresponding concentration. Aalto et al. (2002) considered this expression to analyse tropospheric CO₂ in northern Finland. Secondly, the quadratic equation was employed,

$$y = b_1 + b_2t + b_3t^2, \quad (7)$$

used by Bakwin et al. (1998) to study CO₂ evolution at two sites in North Carolina and Wisconsin. Higher order polynomials were not considered in this study due to their infrequent use. Finally, the exponential relationship was tried.

$$y = c_1 e^{c_2 t}. \quad (8)$$

A similar relationship was employed by Artuso et al. (2009) to investigate the CO₂ trend on the island of Lampedusa.

3. Results

3.1. Monthly evolution

Fig. 2 presents the evolution of both gases by calculations carried out with monthly observations. The yearly cycle is very marked and the increasing trend with time is noticeable for both gases. Extensions of interquartile ranges are more accentuated for CO₂ than for CH₄. Relationships between interquartile range and median were obtained each month and averaged. They were 2.6% for CO₂ and 1.5% for CH₄. Moreover the dispersion of the 90th percentiles is considerably higher for CO₂, implying greater skewness. In fact, the average of Bowley's coefficient, a skewness robust statistic (Pérez et al., 2014) for monthly observations, is 0.25 for CO₂ whereas it was 0.15 for CH₄.

3.2. Decile trends

García et al. (2012) and Pérez et al. (2012) considered the daily evolution for different CO₂ percentiles. Following this approach, deciles of monthly observations were calculated to obtain a

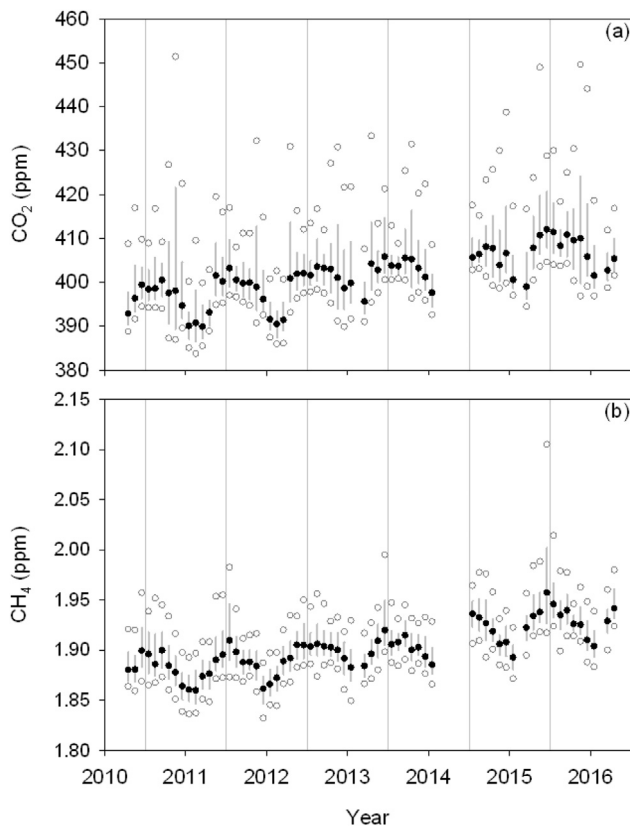


Fig. 2. Evolution of monthly concentrations in the period analysed. Black dots represent the medians, grey lines correspond to the interquartile ranges and empty grey dots are the 10th and 90th percentiles for measurements of CO₂ (a) and CH₄ (b).

detailed estimation of their trend. Coefficients of the three expressions employed are presented in Table 1. Evolutions of a_1 , b_1 and c_1 are similar, and increase when the decile grows. The remaining coefficients only presented a slight change for the highest deciles. Correlation coefficients were similar for the lowest deciles. However, they decreased when the deciles increased for the highest deciles.

Coefficient a_2 represents the growth rate for the linear equation, which is constant with the time in this procedure, reaching 2.24 and $9.6 \cdot 10^{-3}$ ppm year⁻¹ for the CO₂ and CH₄ medians, respectively. Growth rates vary with time in Eqs. (7) and (8).

In the quadratic expression, the growth rate is linear with time, the b_2 coefficient being the initial growth rate. Moreover, since the relationship between b_3 and b_2 is small, this latter coefficient controls the growth rate, and the temporal change of this rate is, in general, slow. The negative value of b_2 for the CH₄ 9th decile indicates an initial decrease in concentration over time. The b_3 coefficient is negative for the six lowest deciles of CO₂ revealing downward concavity of Eq. (7) accompanied by a slight fall in the growth rate equal to $2b_3$ each year. The opposite behaviour is observed for positive values of b_3 , although the increase is greater in this case since the b_3 values are higher. The evolution of the growth rate is extremely marked for CH₄ due to the greater relationship between b_3 and b_2 for this gas.

Coefficient c_2 is so small that Eq. (8) is similar to Eq. (6). In fact, Eq. (8) may be replaced by a Taylor series at $t = 0$ with derivatives of order zero and one, i.e. a straight line where the intercept is c_1 and the slope is $c_1 c_2$, which resemble a_1 and a_2 , respectively. Consequently, the growth rate is given by $c_1 c_2$ in this case.

Although this section focuses on deciles since they are robust statistics, values corresponding to monthly averages are also included in Table 1. They are close to those for the median or deciles slightly above it due to the high outliers that occasionally appear.

3.3. Boundaries of the variables used

Table 2 presents the median of the meteorological variables employed in this analysis, which are a location statistic. Moreover, the 1st and 2nd terciles have been calculated and may be used as frontiers since three intervals can be established. Values below the 1st tercile may be considered low, values between the 1st and the 2nd tercile are medium and, values above the 2nd tercile are high.

Ranges of these intervals depend on the corresponding variable. The second interval for direction, vertical wind speed, potential temperature and pressure is narrow. Differences among these variables depend on their distribution, which is nearly symmetrical for direction, vertical wind speed and potential temperature. However, pressure is left-skewed. Distance, boundary layer height and horizontal wind speed present similar ranges for the first and second intervals, and the distribution of these variables is right-skewed. The final third of distances extends above 1000 km, 1.1% of the boundary layer heights exceed 2000 m and horizontal wind speed may be described by the Weibull distribution with a shape parameter of 1.58 and a scale parameter of 7.6 m s^{-1} . Finally, the recirculation factor is noticeably right-skewed, 2.4% of recirculation factors are above 0.5. Intervals obtained from its terciles are unequal, with their ranges increasing following the value.

Concentrations of gases in the atmosphere depend on various contributions, with meteorological variables playing a key role. From a practical point of view, the strength of the relationship between concentrations and meteorological variables should be quantified. However, as a previous step, the relationship between meteorological variables merits investigation. Table 3 presents correlations between pairs of variables whose coefficients are, in general, satisfactory due to the large number of observations. This

Table 1

Coefficients and correlation coefficient for the equations used to fit the temporal evolution of monthly deciles and averages taking the temporal origin on the first month of the interval.

Gas	Decile	Linear			Quadratic				Exponential		
		a ₁ (ppm)	a ₂ (ppm year ⁻¹)	r	b ₁ (ppm)	b ₂ (ppm year ⁻¹)	b ₃ (ppm year ⁻²)	r	c ₁ (ppm)	c ₂ (year ⁻¹)	r
CO ₂	1	389.50	2.114	0.714	389.21	2.417	-0.051	0.714	389.50	0.0053	0.713
	2	390.89	2.137	0.730	390.55	2.492	-0.059	0.730	390.90	0.0054	0.728
	3	392.15	2.147	0.733	391.78	2.533	-0.065	0.734	392.16	0.0054	0.732
	4	393.45	2.170	0.732	393.18	2.450	-0.047	0.733	393.46	0.0054	0.731
	5	395.00	2.244	0.729	394.85	2.407	-0.027	0.729	395.02	0.0056	0.728
	6	397.05	2.294	0.692	396.98	2.367	-0.012	0.693	397.06	0.0057	0.691
	7	399.81	2.254	0.628	400.22	1.833	0.070	0.629	399.81	0.0055	0.627
	8	403.67	2.405	0.544	404.76	1.274	0.189	0.548	403.65	0.0059	0.545
	9	411.34	2.797	0.428	413.33	0.724	0.347	0.436	411.27	0.0067	0.431
	Average ^a	398.37	2.362	0.676	398.64	2.085	0.046	0.676	398.38	0.0058	0.674
CH ₄	1	1.8506	0.0097	0.779	1.8552	0.0050	0.0008	0.785	1.8507	0.0052	0.778
	2	1.8585	0.0098	0.793	1.8622	0.0060	0.0006	0.797	1.8586	0.0052	0.793
	3	1.8642	0.0098	0.798	1.8684	0.0055	0.0007	0.803	1.8644	0.0052	0.797
	4	1.8692	0.0097	0.789	1.8740	0.0047	0.0008	0.796	1.8693	0.0051	0.789
	5	1.8745	0.0096	0.768	1.8796	0.0043	0.0009	0.776	1.8747	0.0050	0.768
	6	1.8804	0.0095	0.738	1.8860	0.0037	0.0010	0.747	1.8805	0.0049	0.737
	7	1.8879	0.0093	0.698	1.8944	0.0026	0.0011	0.710	1.8880	0.0049	0.698
	8	1.8972	0.0096	0.647	1.9053	0.0012	0.0014	0.664	1.8973	0.0050	0.649
	9	1.9146	0.0098	0.525	1.9263	-0.0023	0.0020	0.551	1.9148	0.0050	0.528
	Average ^a	1.8850	0.0093	0.630	1.8941	-0.0003	0.0016	0.652	1.8851	0.0048	0.630

^a Correspond to the monthly concentration averages.

Table 2

Terciles and medians of the variables used.

Variable	1 st tercile	Median	2 nd tercile
Distance (km)	181.1	261.8	372.9
Direction (degrees)	245.7	280.1	320.7
Recirculation factor	0.019	0.038	0.074
Boundary layer height (m)	337	490	718
Horizontal wind speed (m s ⁻¹)	4.1	5.7	7.9
Vertical wind speed (m s ⁻¹)	-0.0036	-0.0007	0.0022
Potential temperature (K)	290.6	293.6	297.0
Pressure (hPa)	865.7	868.3	870.6

number is over 52,000, with the critical value at a 0.01 significance level being 0.011. Low correlations, whose coefficients were below that value, are marked in italics in Table 3.

Values above 0.400 have been highlighted so as to mark relevant correlations. The greatest values were obtained for distance, followed by horizontal wind speed. The highest correlation revealed that the greater the horizontal wind speed, the greater the distance travelled by the air parcel. The average distance is anti-correlated with potential temperature and the recirculation factor. The noticeable coefficients between average direction and distance or vertical wind speed indicate sinusoidal relationships between the two variables. The best correlation for the boundary layer height was observed with potential temperature. Small values are

obtained for correlations between the recirculation factor and the remaining variables, although a pronounced inverse relationship was observed with horizontal wind speed, which is justified since intense horizontal winds determine straight trajectories and small recirculation factors.

The worst correlation coefficient was obtained between the average distance and vertical wind speed, which do not seem to be correlated, and the second worst corresponded to boundary layer height and pressure.

3.4. Relationship between trend and meteorological variables

The current analysis considers the influence of the meteorological variables previously presented on CO₂ and CH₄ trends. Concentrations were segregated following the terciles of meteorological variables. Together with the correlation coefficient and the change of concentration in the period investigated, coefficients of Eq. (7) were calculated and shown in Table 4.

Coefficient *b*₃ is smaller than *b*₂ for CO₂, which means that the influence of *b*₃ is low at the beginning of the measurement interval, although comparable to *b*₂ at the end. The increase in concentration lies in an interval of around 6 ppm. The concavity of the equation is given by the sign of *b*₃. Since the concentration increase is positive, positive values of *b*₃ reveal a rapid increase at the end of the period, whereas the five negative values of *b*₃ indicate a slow increase at the end of the period. However, this behaviour is barely observed

Table 3

Correlation between pairs of variables.

Variables	r	Variables	r	Variables	r	Variables	r	Variables	r	Variables	r	Variables	r
Dist.-Dir.	0.400	Dir.-R. F.	0.254	R. F.-B. L.	0.083	B. L.-H. W.	-0.165	H. W.-V. W.	0.135	V. W.-P. T.	0.267	P. T.-Pres.	0.301
Dist.-R. F.	-0.452	Dir.-B. L.	0.150	R. F.-H. W.	-0.309	B. L.-V. W.	0.239	H. W.-P. T.	-0.435	V. W.-Pres.	-0.417		
Dist.-B. L.	-0.183	Dir.-H. W.	0.314	R. F.-V. W.	0.034	B. L.-P. T.	0.433	H. W.-Pres.	-0.456				
Dist.-H. W.	0.893	Dir.-V. W.	0.464	R. F.-P. T.	0.210	B. L.-Pres.	<i>-0.010</i>						
Dist.-V. W.	<i>0.007</i>	Dir.-P. T.	0.397	R. F.-Pres.	0.121								
Dist.-P. T.	-0.503	Dir.-Pres.	0.306										
Dist.-Pres.	<i>-0.382</i>												

r, correlation coefficient, square root of Eq. (5) for direction, Dist., average distance, Dir., average direction, R. F., recirculation factor, B. L., boundary layer height, H. W., horizontal wind speed, V. W., vertical wind speed, P. T., potential temperature, Pres., pressure. Bold values are above 0.400 so as to mark relevant correlations.

Table 4
Coefficients for the quadratic fit given by Eq. (7), together with the correlation coefficient, r , and the change in concentration in the 6-year period, Δ .

Variable	Interval	CO ₂				CH ₄					
		b_1 (ppm)	b_2 (ppm y ⁻¹)	b_3 (ppm y ⁻²)	r	Δ (ppm)	b_1 (ppm)	b_2 (ppm y ⁻¹) ^a	b_3 (ppm y ⁻²) ^a	r	Δ (ppm)
Dist.	Low	400.65	1.669	0.121	0.226	14.39	1.8990	-1.936	1.647	0.190	0.0477
	Medium	400.19	1.433	0.144	0.253	13.76	1.8948	0.259	1.457	0.245	0.0540
	High	395.62	2.948	-0.081	0.466	14.76	1.8861	4.402	0.728	0.317	0.0526
Dir.	Low	400.67	1.996	0.133	0.262	16.76	1.9001	-1.792	1.883	0.212	0.0570
	Medium	397.13	2.375	-0.007	0.285	13.99	1.8844	1.097	1.303	0.299	0.0535
	High	398.83	1.425	0.098	0.295	12.08	1.8934	5.580	0.277	0.224	0.0435
R. F.	Low	397.45	1.952	0.079	0.341	14.57	1.8866	2.548	1.080	0.325	0.0542
	Medium	399.55	1.541	0.136	0.266	14.15	1.8954	1.493	1.118	0.192	0.0492
	High	399.75	2.156	0.041	0.241	14.42	1.8971	-0.519	1.510	0.226	0.0512
B. L.	Low	405.49	1.660	0.209	0.268	17.48	1.9156	-0.923	1.511	0.151	0.0488
	Medium	398.77	1.562	0.159	0.336	15.10	1.8915	0.627	1.542	0.343	0.0593
	High	391.23	2.542	-0.033	0.423	14.06	1.8668	5.556	0.646	0.565	0.0566
H. W.	Low	400.59	2.319	-0.011	0.208	13.52	1.8957	1.077	1.082	0.189	0.0454
	Medium	399.85	0.688	0.308	0.288	15.21	1.8969	-5.108	2.490	0.276	0.0590
	High	396.19	2.874	-0.080	0.440	14.37	1.8883	5.414	0.510	0.255	0.0508
V. W.	Low	399.84	1.994	0.038	0.276	13.35	1.8941	4.745	0.653	0.277	0.0520
	Medium	400.24	1.424	0.159	0.248	14.26	1.8998	-0.578	1.383	0.173	0.0463
	High	397.04	1.743	0.144	0.301	15.63	1.8864	-1.893	1.873	0.291	0.0561
P. T.	Low	399.81	1.720	0.120	0.437	14.66	1.9024	3.089	1.030	0.258	0.0556
	Medium	401.35	1.510	0.094	0.214	12.43	1.9036	-4.739	2.094	0.185	0.0469
	High	394.00	2.864	0.020	0.283	17.91	1.8628	7.654	0.541	0.387	0.0654
Pres.	Low	398.41	1.597	0.129	0.361	14.22	1.8948	-0.268	1.500	0.312	0.0524
	Medium	399.25	1.677	0.098	0.228	13.58	1.8946	-2.409	1.777	0.226	0.0495
	High	399.48	1.996	0.093	0.264	15.33	1.8895	6.295	0.441	0.201	0.0536

Bold values correspond to the two highest increases in concentration in the 6-year period for both gases.

^a These coefficients are multiplied by 1000.

due to the low value of b_3 . The lowest increase, around 12 ppm, corresponds to directions from around NW to E, followed by intermediate potential temperatures. However, the greatest increase, nearly 18 ppm, is observed for high potential temperatures, followed by the interval of low boundary layer height values. Consequently, contrasting evolutions appeared with potential temperature, since the increase is small for intermediate values, although large for high ones.

For CH₄, correlation coefficients are, in general, smaller than those for CO₂. Moreover, b_2 and b_3 coefficients are comparable, revealing that the weight of this latter coefficient is noticeable at the end of the measuring interval. Concavity of evolution is positive. However, ten b_2 coefficients are negative, indicating that evolution may even decrease slightly at the beginning of the interval. Concentration changes are also confined in a narrow interval, around 0.016 ppm. The highest and lowest increases were observed in the same variables and intervals as for CO₂. The second highest also corresponded to the boundary layer height, as with CO₂, although for intermediate values. Finally, the second lowest was obtained for small horizontal wind speed values. A contrasting evolution was observed for this variable, since a marked increase was obtained for intermediate values.

The correlation coefficients included in Table 4 are statistically significant, since critical values at the 0.001 level are around 0.028 due to the number of observations, which is nearly 14,000. Consequently, key values are the concentration changes presented in Table 4, since they mark the ranges of every meteorological variable linked to salient concentration increases.

Finally, conditions leading to the two largest increases were combined for the two gases. They are high values of potential temperature, as well as low and medium values of boundary layer height, for CO₂ and CH₄ respectively. The increase, 22 ppm with a standard deviation of 9 ppm, is noticeable for CO₂ although the number of observations is very limited, nearly 7% of available observations, under high potential temperatures together with low boundary layer height values, which appear mainly in summer at

night. The greatest increase for CH₄ is 0.070 ± 0.019 ppm, a little higher than those presented in Table 4. The number of observations for CH₄, in this case under high potential temperature and intermediate boundary layer height, is similar, around 6%, and the period is centred in summer, although it is more extended than for CO₂ and mainly located at the beginning and end of the night.

4. Discussion

4.1. Monthly evolution

Cheng et al. (2017) compared the CO₂ background concentrations measured with flasks to those obtained with the data assimilation system called Carbon Tracker (Peters et al., 2007) at the Waliguan station in China. Although the measurement period extended from March 2009 to December 2010, several features may be highlighted. Firstly, the Carbon Tracker evolution is smoother than the measured one, since the contrast between summer and winter is smaller, and secondly, concentrations from the Carbon Tracker are slightly above the flask concentrations. The main differences are reached in April 2009, when the flask concentration exceeded the Carbon Tracker concentration, although the opposite behaviour appeared in August 2009 and 2010. When this evolution is compared to that presented in Fig. 2, values observed at CIBA are higher than those at Waliguan. Moreover, changes between consecutive months are more pronounced at CIBA, probably due to the features of the semi-natural site where the station is located, which is affected by nearby roads and population centres. This explanation agrees with Rózański et al. (2014), who indicate that spikes and periods of increased concentrations are due to local and/or regional sources. Another salient difference is the sharp contrast between minima reached in summer and adjacent months, which may be attributed to the climate of the region, which is dry and hot in summer when vegetation dies, whereas precipitation in the rest of the year determines vegetation, which mainly grows in spring.

4.2. CO₂ and CH₄ trends

The growth rates calculated in this paper, 2.24 and 9.6 10^{-3} ppm year⁻¹ for the CO₂ and CH₄ monthly medians, respectively, are close to 2.02 ppm year⁻¹ obtained for CO₂ in Central Siberia in the period 2006–2013 (Timokhina et al., 2015) and 0.0074 ppm year⁻¹ for CH₄ at Cabaw, The Netherlands, in the period 2005–2010 (Vermeulen et al., 2011). However, they are far from the 3.8 ppm year⁻¹ for CO₂ recorded at Shangdianzi, China, under the Beijing-Tianjin-Hebei influence (Fang et al., 2016) and around 0.017 ppm year⁻¹ for CH₄ observed at Hegyhátsál, Hungary (Haszpra et al., 2011).

Second order polynomials have scarcely been used, noticeable examples being Bakwin et al. (1998) and Fang et al. (2016). Unfortunately, a detailed analysis of coefficients was not included in these studies. Róžański et al. (2014) presented smoothed curves, use of which is frequent, to indicate the evolution of greenhouse gases and selected halocarbons at a Polish station. These curves are suitable for large datasets since they mark periods which display growth that is different to that usually found at the site. However, for short series of observations, simpler equations, such as those considered in this study, provide an accurate description of the evolution.

4.3. Correlation between pairs of meteorological variables

When analysing correlations between meteorological variables it should not be forgotten that they do not evolve independently, since they are linked by atmospheric cycles. This is the case of negative correlations between distance and potential temperature or recirculation factor. When temperatures are high, in summer, wind speed is low and the average distance is small. Similarly, large recirculation factors are linked to stagnant conditions and low distances.

The analysis of correlation coefficients for the direction reveals the sinusoidal relationships with distance and vertical wind speed. Distances are small from around E to S and large from around SW to NW, as reported in a previous study based on a three-year analysis (Pérez et al., 2015b). The directional cycle for vertical wind speed is noticeable since the lowest values are obtained from around N to NE and the highest from around SW to W.

The satisfactory correlation between the boundary layer height and the potential temperature is explained by two cycles. The annual cycle features the noticeable development of the boundary layer in summer in agreement with temperature (Pérez et al., 2016), and the daily cycle shows small values of both variables at night. Guo et al. (2016) investigated the climatology of the planetary boundary layer height in China and concluded its negative association with surface pressure and lower troposphere stability and its positive association with near-surface wind speed and temperature. In agreement with this research, the correlation between boundary layer height and pressure is slightly negative, although variables used in this paper correspond to 500 m a.g.l. This low negative value is due to the daily cycle, since the greatest heights of the boundary layer, above 2000 m, are obtained with large pressures during the daytime. However, the lowest boundary layer heights are mainly observed during the night over a wide pressure interval.

The annual cycle also justifies different correlations, such as the negative value obtained for horizontal wind speed with potential temperature, since temperature is high in summer when horizontal wind speed is low, and is the opposite in winter. Similarly, this cycle explains the negative correlations of both horizontal and vertical wind speed with pressure. In winter, low pressure systems sweep the Iberian Peninsula causing high horizontal wind speed and high

vertical wind speed, and the opposite in summer. Finally, the correlation between potential temperature and pressure, which is not very small, may be understood with the annual cycle of both variables.

4.4. Trends and meteorological variables

Few studies present the close relationship between meteorological variables and CO₂ concentration in the boundary layer, such as the analysis of Li et al. (2014) focusing on vertical profiles, which are related with atmospheric boundary layer depth and atmospheric stability. Another example is the study of Sánchez et al. (2010), which shows that strong inversions of up to 7.5 °C per 100 m at CIBA contribute to trapping CO₂ in the lowest atmosphere during night-time. Although a climatology of air pollution has occasionally been presented (Buchholz et al., 2016), the influence of meteorological variables on CO₂ and CH₄ trends has scarcely been investigated. One prominent example is the analysis suggested by Zhang et al. (2013), which studied CO₂ at Mount Waliguan Baseline Observatory, western China, between 1995 and 2008. They mainly focused on sources, sinks and their changes, and viewed meteorological conditions as a secondary consideration. However, the current study highlights the fact that CO₂ and CH₄ increases are closely linked to meteorological conditions. In particular, boundary layer height and potential temperature are key variables in CO₂ and CH₄ evolution.

5. Conclusions

Analysis of monthly CO₂ and CH₄ observations revealed the greater dispersion of CO₂ measurements, which were also more skewed than CH₄ data.

Linear analysis of monthly deciles provided rates of 2.14 and 9.6 10^{-3} ppm year⁻¹ for the CO₂ and CH₄ medians respectively. The quadratic equation used with these deciles revealed a decrease in the rise of CO₂ when time increased for the lowest deciles, although the rate increased with time for the remaining deciles and for CH₄. The exponential equation was also considered, although the evolution described with this expression was similar to the linear evolution.

Terciles of meteorological variables were proposed as boundaries. Three groups of variables were created, the first, formed by wind direction, vertical wind speed, potential temperature and pressure, presents a narrow interval between the first and second terciles. The second group is formed by the distance, boundary layer height and horizontal wind speed, whose intervals below the first tercile and between the first and the second tercile were similar. The recirculation factor shows three unequal intervals. As regards skewness, pressure is left-skewed, whereas distance, boundary layer height, horizontal wind speed and recirculation factor are right-skewed.

The link between meteorological variables was quantified. The greatest correlation coefficient was obtained between distance and horizontal wind speed, since large distances are associated with high horizontal wind speeds. Noticeable anti-correlations are observed between potential temperature with distance and horizontal wind speed and between pressure with horizontal and vertical wind speeds, which may be linked with the annual cycle, since both temperature and pressure are higher in summer. Wind direction is correlated with distance and vertical wind speed, revealing a sinusoidal relationship between the two variables.

The quadratic evolution was analysed in the intervals of meteorological variables. The greatest CO₂ increase was obtained for high potential temperatures (above 297 K) followed by low boundary layer heights (below 337 m). For CH₄, the greatest

increase was also observed for high potential temperatures, although followed by intermediate boundary layer heights (between 337 and 718 m). Both meteorological variables were combined to calculate the resulting increase, which was around 22 ± 9 and 0.070 ± 0.019 ppm for CO₂ and CH₄, respectively, although the number of observations was very limited, around 7%, and were in summer, at night for CO₂, and at the beginning and end of the night for CH₄.

As a final conclusion, certain meteorological variables, high values of potential temperature and low or medium values of boundary layer height for CO₂ and CH₄ respectively, strongly impact on the evolution of concentrations and should not be excluded when providing a comprehensive description of the two gases.

Conflict of interests

The authors declare no conflict of interests regarding publication of this paper.

Acknowledgements

The authors wish to acknowledge the financial support of the Ministry of Economy and Competitiveness and ERDF funds (project numbers CGL2009-11979 and CGL2014-53948-P).

References

- Aalto, T., Hatakka, J., Paatero, I., Tuovinen, J.P., Aurela, M., Laurila, T., Holmén, K., Trivett, N., Viisanen, Y., 2002. Tropospheric carbon dioxide concentrations at a northern boreal site in Finland: basic variations and source areas. *Tellus Ser. B-Chem. Phys. Meteorol.* 54, 110–126. <https://doi.org/10.1034/j.1600-0889.2002.00297.x>.
- Abuzaid, A.H., Mohamed, I.B., Hussin, A.G., 2012. Boxplot for circular variables. *Comput. Stat.* 27, 381–392. <https://doi.org/10.1007/s00180-011-0261-5>.
- Allwine, K.J., Whiteman, C.D., 1994. Single-station integral measures of atmospheric stagnation, recirculation and ventilation. *Atmos. Environ.* 28, 713–721. [https://doi.org/10.1016/j.1352-2310\(94\)90048-5](https://doi.org/10.1016/j.1352-2310(94)90048-5).
- Angelbratt, J., Mellqvist, J., Blumenstock, T., Borsdorff, T., Brohede, S., Duchatelet, P., Forster, F., Hase, F., Mahieu, E., Murtagh, D., Petersen, A.K., Schneider, M., Sussmann, R., Urban, J., 2011. A new method to detect long term trends of methane (CH₄) and nitrous oxide (N₂O) total columns measured within the NDACC ground-based high resolution solar FTIR network. *Atmos. Chem. Phys.* 11, 6167–6183. <https://doi.org/10.5194/acp-11-6167-2011>.
- Artuso, F., Chamard, P., Piacentino, S., Sferlazzo, D.M., De Sarra, A., Meloni, D., Monteleone, F., 2009. Influence of transport and trends in atmospheric CO₂ at Lampedusa. *Atmos. Environ.* 43, 3044–3051. <https://doi.org/10.1016/j.atmosenv.2009.03.027>.
- Bakwin, P.S., Tans, P.P., Hurst, D.F., Zhao, C., 1998. Measurements of carbon dioxide on very tall towers: results of the NOAA/CMDL program. *Tellus Ser. B-Chem. Phys. Meteorol.* 50, 401–415.
- Buchholz, R.R., Paton-Walsh, C., Griffith, D.W.T., Kubistin, D., Caldow, C., Fisher, J.A., Deutscher, N.M., Kettlewell, G., Riggenbach, M., Macatangay, R., Krummel, P.B., Langenfelds, R.L., 2016. Source and meteorological influences on air quality (CO, CH₄ & CO₂) at a Southern Hemisphere urban site. *Atmos. Environ.* 126, 274–289. <https://doi.org/10.1016/j.atmosenv.2015.11.041>.
- CGER, 2017. <http://db.cger.nies.go.jp/metex/trajectory.html> (accessed 3 November 2017).
- Cheng, S., An, X., Zhou, L., Tans, P.P., Jacobson, A., 2017. Atmospheric CO₂ at Waliguan station in China: transport climatology, temporal patterns and source-sink region representativeness. *Atmos. Environ.* 159, 107–116. <https://doi.org/10.1016/j.atmosenv.2017.03.055>.
- Eneroth, K., Aalto, T., Hatakka, J., Holmén, K., Laurila, T., Viisanen, Y., 2005. Atmospheric transport of carbon dioxide to a baseline monitoring station in northern Finland. *Tellus Ser. B-Chem. Phys. Meteorol.* 57, 366–374. <https://doi.org/10.1111/j.1600-0889.2005.00160.x>.
- Fang, S.X., Tans, P.P., Dong, F., Zhou, H., Luan, T., 2016. Characteristics of atmospheric CO₂ and CH₄ at the Shangdianzi regional background station in China. *Atmos. Environ.* 131, 1–8. <https://doi.org/10.1016/j.atmosenv.2016.01.044>.
- Fernández-Duque, B., Pérez, I.A., Sánchez, M.L., García, M.A., Pardo, N., 2017. Temporal patterns of CO₂ and CH₄ in a rural area in northern Spain described by a harmonic equation over 2010–2016. *Sci. Total Environ.* 593–594, 1–9. <https://doi.org/10.1016/j.scitotenv.2017.03.132>.
- Fisher, N.I., 1993. *Statistical Analysis of Circular Data*. Cambridge University Press, Cambridge.
- García, M.A., Sánchez, M.L., Pérez, I.A., 2012. Differences between carbon dioxide levels over suburban and rural sites in Northern Spain. *Environ. Sci. Pollut. Res.* 19, 432–439. <https://doi.org/10.1007/s11356-011-0575-4>.
- Grant, E.R., Ross, A.N., Gardiner, B.A., Mobbs, S.D., 2015. Field observations of canopy flows over complex terrain. *Bound.-Layer Meteorol.* 156, 231–251. <https://doi.org/10.1007/s10546-015-0015-y>.
- Guo, J., Miao, Y., Zhang, Y., Liu, H., Li, Z., Zhang, W., He, J., Lou, M., Yan, Y., Bian, L., Zhai, P., 2016. The climatology of planetary boundary layer height in China derived from radiosonde and reanalysis data. *Atmos. Chem. Phys.* 16, 13309–13319. <https://doi.org/10.5194/acp-16-13309-2016>.
- Haszpra, L., Barcza, Z., Szilágyi, I., Dlugokencky, E., Tans, P., 2011. Trends and temporal variations of major greenhouse gases at a rural site in central Europe. In: Haszpra, L. (Ed.), *Atmospheric Greenhouse Gases: the Hungarian Perspective*. Springer, Dordrecht, pp. 29–47. https://doi.org/10.1007/978-90-481-9950-1_3.
- Hernández-Paniagua, I.Y., Lowry, D., Clemishaw, K.C., Fisher, R.E., France, J.L., Lanoisellé, M., Ramonet, M., Nisbet, E.G., 2015. Diurnal, seasonal, and annual trends in atmospheric CO₂ at southwest London during 2000–2012: wind sector analysis and comparison with Mace Head, Ireland. *Atmos. Environ.* 105, 138–147. <https://doi.org/10.1016/j.atmosenv.2015.01.021>.
- Inoue, H.Y., Matsueda, H., Igarashi, Y., Sawa, Y., Wada, A., Nemoto, K., Sartorius, H., Schlosser, C., 2006. Seasonal and long-term variations in atmospheric CO₂ and ⁸⁵Kr in Tsukuba, central Japan. *J. Meteorol. Soc. Jpn.* 84, 959–968. <https://doi.org/10.2151/jmsj.84.959>.
- Kutter, E., Yi, C., Hendrey, G., Liu, H., Eaton, T., Ni-Meister, W., 2017. Recirculation over complex terrain. *J. Geophys. Res. Atmos.* 122, 6637–6651. <https://doi.org/10.1002/2016JD026409>.
- Li, Y., Deng, J., Mu, C., Xing, Z., Du, K., 2014. Vertical distribution of CO₂ in the atmospheric boundary layer: characteristics and impact of meteorological variables. *Atmos. Environ.* 91, 110–117. <https://doi.org/10.1016/j.atmosenv.2014.03.067>.
- Mardia, K.V., 1976. *Linear circular correlation coefficients and rhythmometry*. *Biometrika* 63, 403–405.
- NOAA, 2017. <http://ready.arl.noaa.gov/HYSPLIT.php> (accessed 3 November 2017).
- Nomura, S., Mukai, H., Terao, Y., Machida, T., Nojiri, Y., 2017. Six years of atmospheric CO₂ observations at Mt. Fuji recorded with a battery-powered measurement system. *Atmos. Meas. Tech.* 10, 667–680. <https://doi.org/10.5194/amt-10-667-2017>.
- Pérez, I.A., Artuso, F., Mahmud, M., Kulshrestha, U., Sánchez, M.L., García, M.A., 2015a. Applications of air mass trajectories. *Adv. Meteorol.* 2015, 284213. <https://doi.org/10.1155/2015/284213>.
- Pérez, I.A., Sánchez, M.L., García, M.A., Ozores, M., Pardo, N., 2014. Analysis of carbon dioxide concentration skewness at a rural site. *Sci. Total Environ.* 476–477, 158–164. <https://doi.org/10.1016/j.scitotenv.2014.01.019>.
- Pérez, I.A., Sánchez, M.L., García, M.A., Pardo, N., 2012. Analysis of CO₂ daily cycle in the low atmosphere at a rural site. *Sci. Total Environ.* 431, 286–292. <https://doi.org/10.1016/j.scitotenv.2012.05.067>.
- Pérez, I.A., Sánchez, M.L., García, M.A., Pardo, N., 2015b. Analysis of air mass trajectories in the northern plateau of the Iberian Peninsula. *J. Atmos. Sol. Terr. Phys.* 134, 9–21. <https://doi.org/10.1016/j.jastp.2015.09.003>.
- Pérez, I.A., Sánchez, M.L., García, M.A., Pardo, N., 2016. Features of the annual evolution of CO₂ and CH₄ in the atmosphere of a Mediterranean climate site studied using a nonparametric and a harmonic function. *Atmos. Pollut. Res.* 7, 1013–1021. <https://doi.org/10.1016/j.apr.2016.06.006>.
- Pérez, I.A., Sánchez, M.L., García, M.A., Pardo, N., 2017. Trend analysis of CO₂ and CH₄ recorded at a semi-natural site in the northern plateau of the Iberian Peninsula. *Atmos. Environ.* 151, 24–33. <https://doi.org/10.1016/j.atmosenv.2016.11.068>.
- Peters, W., Jacobson, A.R., Sweeney, C., Andrews, A.E., Conway, T.J., Masarie, K., Miller, J.B., Bruhwiler, L.M.P., Pétron, G., Hirsch, A.I., Worthy, D.E.J., Van Der Werf, G.R., Randerson, J.T., Wennberg, P.O., Krol, M.C., Tans, P.P., 2007. An atmospheric perspective on North American carbon dioxide exchange: Carbon-Tracker. *Proc. Natl. Acad. Sci. U. S. A.* 104, 18925–18930. <https://doi.org/10.1073/pnas.0708986104>.
- Rózański, K., Nećki, J., Chmura, Ł., Śliwka, Ł., Zimnoch, M., Bielewski, J., Gaikowski, M., Bartyzel, J., Rosiek, J., 2014. Anthropogenic changes of CO₂, CH₄, N₂O, CFCl₃, CF₂Cl₂, CCl₂FCClF₂, CHCl₃, CH₃CCl₃, CCl₄, SF₆ and SF₅CF₃ mixing ratios in the atmosphere over southern Poland. *Geol. Q.* 58, 673–684. <https://doi.org/10.7306/gq.1153>.
- Sánchez, M.L., Pérez, I.A., García, M.A., 2010. Study of CO₂ variability at different temporal scales recorded in a rural Spanish site. *Agric. For. Meteorol.* 150, 1168–1173. <https://doi.org/10.1016/j.agrformet.2010.04.018>.
- Snyder, J.P., 1987. *Map Projections – a Working Manual*. U.S. Government Printing Office, Washington.
- Sreenivas, G., Mahesh, P., Subin, J., Lakshmi Kanchana, A., Venkata Narasimha Rao, P., Kumar Dadhwal, V., 2016. Influence of meteorology and interrelationship with greenhouse gases (CO₂ and CH₄) at a suburban site of India. *Atmos. Chem. Phys.* 16, 3953–3967. <https://doi.org/10.5194/acp-16-3953-2016>.
- Timokhina, A.V., Prokushkin, A.S., Onuchin, A.A., Panov, A.V., Kofman, G.B., Verkhovets, S.V., Heimann, M., 2015. Long-term trend in CO₂ concentration in the surface atmosphere over Central Siberia. *Russ. Meteorol. Hydrol.* 40, 186–190. <https://doi.org/10.3103/S106837391503005X>.
- Vermeulen, A.T., Hensen, A., Popa, M.E., Van Den Bulk, W.C.M., Jongejan, P.A.C., 2011. Greenhouse gas observations from Cabauw Tall Tower (1992–2010). *Atmos. Meas. Tech.* 4, 617–644. <https://doi.org/10.5194/amt-4-617-2011>.
- Wharton, S., Ma, S., Baldocchi, D.D., Falk, M., Newman, J.F., Osuna, J.L., Bible, K., 2017. Influence of regional nighttime atmospheric regimes on canopy turbulence and gradients at a closed and open forest in mountain-valley terrain. *Agric. For.*

- Meteorol. 237–238, 18–29. <https://doi.org/10.1016/j.agrformet.2017.01.020>.
- WDCGG (World Data Centre for Greenhouse Gases), 2017. <http://ds.data.jma.go.jp/gmd/wdogg/>(accessed 11 May 2017).
- Wu, J., Guan, D., Yuan, F., Yang, H., Wang, A., Jin, C., 2012. Evolution of atmospheric carbon dioxide concentration at different temporal scales recorded in a tall forest. *Atmos. Environ.* 61, 9–14. <https://doi.org/10.1016/j.atmosenv.2012.07.013>.
- Zeng, J., Matsunaga, T., Mukai, H., 2010. METEX - a flexible tool for air trajectory calculation. *Environ. Modell. Softw.* 25, 607–608. <https://doi.org/10.1016/j.envsoft.2008.10.015>.
- Zhang, F., Zhou, L., Conway, T.J., Tans, P.P., Wang, Y., 2013. Short-term variations of atmospheric CO₂ and dominant causes in summer and winter: analysis of 14-year continuous observational data at Waliguan, China. *Atmos. Environ.* 77, 140–148. <https://doi.org/10.1016/j.atmosenv.2013.04.067>.